

# Mobility edge for cold atoms in laser speckle potentials

Dominique Delande<sup>1</sup> and Giuliano Orso<sup>2</sup>

<sup>1</sup>*Laboratoire Kastler Brossel, UPMC-Paris6, ENS, CNRS; 4 Place Jussieu, F-75005 Paris, France*

<sup>2</sup>*Laboratoire Matériaux et Phénomènes Quantiques, Université Paris Diderot-Paris 7 and CNRS, UMR 7162, 75205 Paris Cedex 13, France*

(Dated: December 3, 2024)

Based on the transfer matrix method, we numerically compute the precise position of the mobility edge of atoms exposed to a laser speckle potential. Our results deviate significantly from previous theoretical estimates using an approximate self-consistent approach of localization and we explain the origin of the discrepancy. In particular we find that the position of the mobility edge in blue-detuned speckles is much below than in the red-detuned counterpart, pointing out the crucial role played by the asymmetric on-site distribution of speckle patterns.

PACS numbers: 03.75.-b, 05.30.Rt, 64.70.Tg, 05.60.Gg

Anderson localization (AL), namely the absence of diffusion of waves in certain disordered media, is a ubiquitous phenomenon originating from the interference of multiple scatterings from random defects [1, 2]. Among others, AL has been reported for light waves in diffusive media [3, 4] or photonic crystals [5, 6], sound waves [7], microwaves [8]. Cold atomic gases do have very appealing properties for studying AL: interference effects can be preserved over a relatively long time, atom-atom interaction effects are small thanks to the absence of Coulomb interaction and can be controlled using e.g. Feshbach resonances. Last, but not least, the spatial and temporal typical scales are convenient for a direct observation of the localization effect, starting from an initially localized wavepacket and monitoring its expansion vs. time.

The dimension of the system is a crucial parameter. In dimension 1 (1D) and 2, AL is the generic scenario and it was indeed possible to directly observe AL of 1D atomic Bose gases [9, 10]. In dimension three (3D) and above, there is a metal-insulator transition at a specific energy  $E = E_c$ , the so-called mobility edge, separating localized ( $E < E_c$ ) from diffusive ( $E > E_c$ ) states. Interestingly, the kicked rotor model describing cold atoms exposed to a periodic or quasi-periodic sequence of far-detuned laser pulses can be mapped to an Anderson model in momentum space. This made it possible to observe 1D AL in momentum space [11] as early as 1995. More recently, the 3D Anderson transition has been experimentally observed [12], the critical exponent accurately measured and its universality tested [13].

Experiments on 3D AL in configuration space, using a laser speckle potential as a source of disorder for atoms, are less advanced. The reasons are twofold. First the broad-band energy distribution of the expanding atoms severely complicates the extraction of the position of the mobility edge from the raw data. Second and most important, a direct comparison with theory remains problematic. On one hand the position of the experimentally measured [14] mobility edge in highly anisotropic speckle patterns is unexpectedly high compared to the

best available [15, 16] theoretical estimates based on an approximate theory, called the self-consistent theory of localization (SCTL) [17]. On the other hand, for more isotropic correlations, the experimentally measured [18] position of the mobility edge is instead significantly lower than expected from theory [19].

Differently from typical condensed matter systems, the on-site distribution  $P(V)$  of the blue-detuned speckles employed in both experiments [14, 18] is not Gaussian, but follows a Poissonian law [20]:

$$P(V) = \frac{\Theta(V + V_0)}{V_0} \exp\left(-\frac{V + V_0}{V_0}\right) \quad (1)$$

where  $\Theta$  is the Heaviside function and  $V_0$  is related to the variance by  $\langle V^2 \rangle = V_0^2$ . For later convenience, here we have shifted the potential by its average value. The distribution for the red-detuned speckle can be obtained from Eq.(1) under the change  $V \rightarrow -V$ .

In this Letter we use the transfer matrix technique together with the finite-size scaling to pinpoint the precise position of the mobility edge for massive particles in laser speckle potentials. We show that *i*) for blue-detuned speckle, the previous theoretical calculations based on the SCTL significantly overestimate the correct position of the mobility edge; *ii*) the values of  $E_c$  for red and blue speckles are completely different due to the asymmetry  $P(V) \neq P(-V)$  of the distribution (1), while the current implementations of the SCTL would predict the same value; *iii*) at least for isotropic speckles, the position of the mobility edge depends mainly on the width of the correlation function  $\langle V(0)V(\mathbf{r}) \rangle$  of the potential rather than on its specific shape.

The transfer matrix method, first used to study the 3D Anderson model [21, 22], represents one of the most powerful numerical technique to compute the exact position of the mobility edge for disordered lattice models. Hence, our starting point is to spatially discretize the continuous Schrödinger equation on a cubic grid: the Laplace operator is replaced by a 7 points (central point + 6 nearest neighbors) sum corresponding to an effective hopping

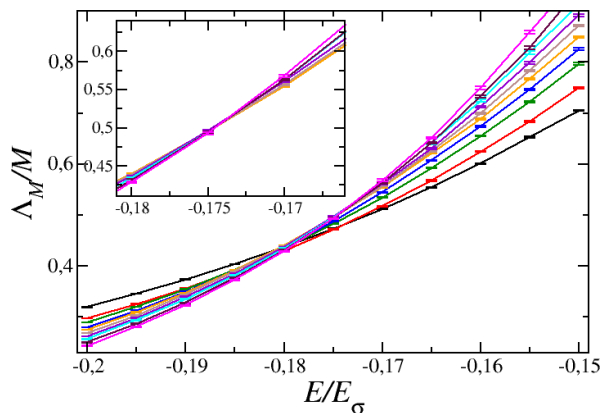


FIG. 1: (color online) Numerical determination of the mobility edge of a cold atom in a disordered 3D potential created by a blue-detuned speckle with scaled strength  $V_0 = 0.5E_\sigma$ . For a given energy, we compute the localization length  $\Lambda_M$  of a long bar-shaped grid with square section  $M \times M$ . Each curve is computed for a single  $M$  value and shows  $\Lambda_M/M$  vs. energy. The various curves cross at the position of the mobility edge. The main plot includes curves from  $M = 35$  (less steep, black curve) to  $M = 80$  (steepest magenta curve), that suggest a mobility edge around  $-0.18E_\sigma$ . When only the largest  $M$  values are kept – in the inset – a better estimate  $E_c = -0.173E_\sigma$  is obtained.

rate  $J = \hbar^2/(2m\Delta^2)$ , where  $\Delta$  is the discretization step. The energy  $E$ , with  $E \ll J$  is measured with respect to the bottom of the band,  $-6J$ .

The disordered potential at each site is generated by properly convoluting a  $\delta$ -correlated random sequence in order to reproduce at the same time the on-site potential distribution  $P(V)$  and the desired correlation function [20, 23]. We first consider the case of a blue speckle, whose distribution is given by Eq. (1). Following [15, 16, 24], we chose the simplest case of a speckle created by a statistically isotropic 3D illumination, with correlation function:

$$\langle V(\mathbf{r}')V(\mathbf{r}' + \mathbf{r}) \rangle = V_0^2 C^2(r/\sigma) \quad (2)$$

where  $C(r) = \sin r/r$  and  $\sigma$  is the characteristic correlation length. The associated "correlation" energy sets the important energy scale of the problem:

$$E_\sigma = \frac{\hbar^2}{m\sigma^2} \quad (3)$$

where  $m$  is the mass of the atom. In the following we measured all energies in units of  $E_\sigma$ . The discretization step must be chosen sufficiently small to resolve the details of the disordered potential and the oscillations of the wavefunction, that is smaller than  $\sigma$  and the de Broglie wavelength. When  $V_0$  and  $E$  are of the order of unity, the de Broglie wavelength is of the order of  $2\pi\sigma$ . We have thus chosen a discretization step  $\Delta = 0.2\pi\sigma$ . We have carefully checked that, up to  $V_0 = 1$ , the discretization

error on the determination of the mobility edge is smaller than 0.005 (of the order of 0.001 at  $V_0 = 0.5$ ).

The basic idea of the transfer matrix method is to compute the total transmission of a bar-shaped grid with length  $L$  and square transverse section  $M \times M$ . Periodic boundary conditions are used in the transverse directions. When the length of the bar is much larger than its transverse size,  $L \gg M$ , the system can be viewed as a quasi-1D and will thus be Anderson localized: its total transmission which can be recursively computed using either the transfer matrix method or equivalently the recursive Green's function method, decays like  $\exp(-2L/\Lambda_M)$  where  $\Lambda_M$  is the quasi-1D localization length in units of the lattice spacing. In practice, the log of the total transmission is a self-averaging quantity which can be safely computed, together with error bars, by using either very long bars or smaller ones but averaging over many independent realizations of the disorder.

$\Lambda_M$  depends on  $M$ , but also on the energy and on the strength of the disorder. Figure 1 shows the ratio  $\Lambda_M/M$  as a function of energy, for various  $M$  values, at a fixed disorder strength  $V_0 = 0.5$ . At low energy,  $\Lambda_M/M$  decreases with  $M$  and eventually behaves like  $\Lambda_\infty/M$  when  $M \rightarrow \infty$ , where  $\Delta\Lambda_\infty$  is the 3D "true" localization length: this is the localized regime. In contrast, at high energy,  $\Lambda_M/M$  increases with  $M$  (proportionally to  $M$  when  $M \rightarrow \infty$ ), a signature of the diffusive regime. At the mobility edge,  $\Lambda_M/M$  is a constant of order unity, meaning that the quasi-1D localization length is comparable to the transverse size of the system, a signature of marginal 3D localization with  $\Lambda_\infty \rightarrow \infty$ . Thus, the mobility edge can be obtained by looking at the point where all curves cross in Fig. 1. For small  $M$ , finite-size effects are rather important and the crossing is not perfect: looking at only the lowest  $M$ , one could get the false impression that the crossing takes place at  $E = -0.18$ , while the highest  $M$  values (inset) show that the true crossing is at  $E = -0.173 \pm 0.002$ . Reaching such a high precision in the determination of the mobility edge requires massive computing resources: transverse system size up to  $M = 80$ , thus transfer matrices of size up to  $2M^2 = 12800$ , longitudinal size of the bar up to 1 million sites. Altogether, data shown in Fig. 1 required 200 000 hours of computation on a supercomputer with slightly more than  $10^{19}$  arithmetic operations. For the 3D Anderson model with *uncorrelated* disorder, the same accuracy can be reached with much smaller transverse sizes, say  $M = 20 - 25$ .

Finite-size scaling is a technique making it possible to go beyond the visual detection of the crossing, but pinpointing more accurately the position of the mobility edge as well as the critical exponent associated with the algebraic divergence of the localization length on the insulating side of the Anderson transition (and its partner, the algebraic vanishing of the diffusion constant on the diffusive side). We have used this technique –

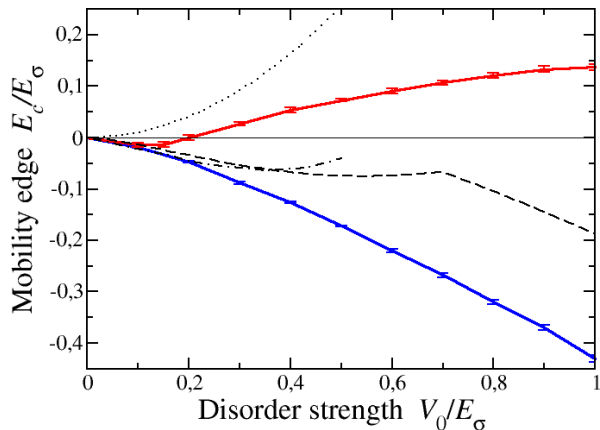


FIG. 2: (color online) Mobility edge separating localized atoms (at low energy) from diffusive atoms (at high energy) for cold atoms in a disordered 3D speckle potential. Energies are measured in units of the correlation energy  $E_\sigma$ , Eq. (3). The solid lines (lower, blue curve and upper, red curve) correspond respectively to blue and red detuned speckles. While the former mobility edge lies always below the average potential (shown by the horizontal thin line), the latter becomes positive as the potential strength increases. The dotted line shows the prediction of the naive self-consistent theory of localization [24]. The dashed dash-dotted lines are the predictions of improved self-consistent theories incorporating the real part of the self-energy [15, 16] which nevertheless lie rather far from the exact numerical results and fail to predict the large difference between blue and red speckles.

which is tantamount to perform the  $M \rightarrow \infty$  extrapolation – to confirm the position of the mobility edge at  $E_c = -0.172 \pm 0.0015$ . However, the presence of strong finite size corrections, originating from the finite correlation length of the potential and causing the fake crossing in Fig. 1, makes the  $M \rightarrow \infty$  extrapolation much more difficult. A conservative estimate of the critical exponent gives  $\nu = 1.6 \pm 0.2$ , much less accurate but fully compatible with the value  $\nu = 1.571 \pm 0.008$  obtained for the Anderson model [22].

We repeat the same calculation for various values of the potential strength. To save computer resources, we use smaller system sizes, resulting in slightly larger error bars on the position of the mobility edge, but always smaller than  $0.01E_\sigma$ . The obtained results for the blue speckle are shown in Fig. 2 by the blue solid line, together with the small error bars. We see from Fig. 2 that, for the blue speckle, the mobility edge is negative for all disorder strength  $V_0$ ; in other words, the mobility edge always lies *below* the average potential.

We also perform analogous calculations for a red speckle, but keeping the spatial correlation function of the disorder, Eq. (2) unchanged. This is shown in Fig. 2 by the red solid line. We see that for small disorder strengths, the mobility edges of red and blue speckles are both negative and very close to each other, but for

Correlation function $C(r)$ , eq. (2)	Blue-detuned mobility edge	Red-detuned mobility edge
$\sin r/r$	-0.172(2)	0.073(2)
$\exp(-r^2/4)$	-0.181(4)	0.054(4)
$3(\sin r/r - \cos r)/r^2$	-0.175(5)	0.053(8)

TABLE I: Mobility edge for various disordered speckle potentials, all calculated for  $V_0/E_\sigma = 0.5$ . The various potentials correspond to different spatial correlation functions, adjusted to have the same width at half-maximum. The mobility edge is computed both for the blue-detuned (positive detuning) and the red-detuned (negative detuning) cases. Digits in parenthesis is the uncertainty on the last digit. The most important factor is the sign of the detuning, while the precise form of the spatial correlation function has only a small effect on the position of the mobility edge.

stronger disorder  $V_0 \gtrsim 0.2$  the mobility edge of the red speckle becomes positive and lies well above the blue one.

Let us now compare our precise numerical results with the three available [15, 16, 24] theoretical estimates based on different implementations of the SCTL. These are shown in Fig. 2 by, respectively, the dotted, the dot-dashed and the dashed lines. Despite the SCTL is an approximate theory it turned out to be surprisingly good for simple models such as the Anderson model [25]. The SCTL was naively applied to speckles in [24] assuming that the spectral function and the density of states are unaffected by the disorder. The prediction of this (on-shell) approximation is that the mobility edge is always positive, see Fig. 2, and is obviously rather bad.

A simple attempt to cure this problem is to incorporate in the SCTL the real part of the self-energy, which shifts the effective lower bound of the spectrum to negative energies [28]. Two variants of this simple idea have been used [15, 16], predicting that the mobility edge of the blue speckle is actually negative. However we see in Fig. 2 that these theories become rapidly inaccurate as the disorder strength increases. First, they significantly overestimate the correct position of the mobility edge. Second, in these theories the scattering amplitude is still evaluated at the lowest (i.e. second) order in the Born approximation, making the mobility edge dependent only on the correlation function, Eq. (2), but not on the potential distribution, Eq. (1). As a consequence the SCTL predicts *identical* mobility edges for blue and red speckles, which is clearly incorrect.

In order to identify the origin of this failure, we use different models of disordered potentials. In table I, we show the values of the mobility edges at  $V_0 = 0.5$ , for red and blue speckles, with various isotropic correlation functions  $C(r)$  (the third one was adopted in Refs.[26, 27]). In order to make the comparison meaningful, we have adjusted the parameter  $\sigma$  for the potential correlation function to reproduce the same width at half-maximum in the 3 cases, keeping of course the same strength  $V_0$

Correlation function $C(r)$	Mobility edge
$\sin r/r$	-0.135(5)
$\exp(-r^2/4)$	-0.124(4)

TABLE II: Mobility edge for Gaussian distributed disordered potentials, calculated for  $V_0/E_\sigma = 0.5$ , and two different spatial correlation functions. The mobility edge is between the blue and red results in table I, confirming that the potential distribution is the important factor. Conversely, the precise form of the spatial correlation function has only a small effect.

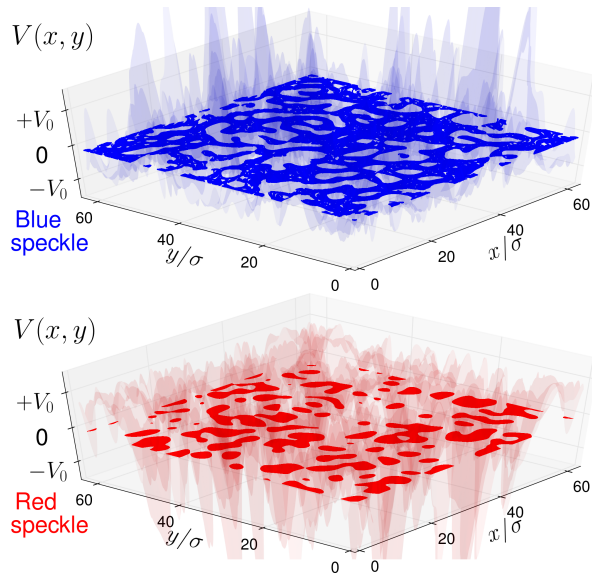


FIG. 3: (color online) Planar cuts in color: classically allowed regions in the transverse section of the grid at energy  $-0.15V_0$  (transparent regions are classically forbidden). The allowed region for the blue speckle is very well connected while it is disconnected for the red speckle.

of the potential. As can be seen in table I, the mobility edges are almost identical for the 3 blue speckles, around -0.175, and almost identical for the 3 red speckles, around +0.06. This proves that the essential ingredient which determines the mobility edge is the distribution  $P(V)$  of disorder strength. This can be *qualitatively* understood using a percolation argument. Figure 3 shows the classically available regions on a given transverse section of the grid,  $V(x, y, z = z_0) < E$ , for a blue and a red speckle at the same energy  $E = -0.15V_0$ , roughly half-way between the two mobility edges. We see that the blue region is strongly connected – which favors delocalization – while the red region is composed of disconnected islands.

The details of the potential correlation function just give rise to small variations of the mobility edge. The physical picture is that, at the mobility edge, the disorder is so strong that all orders of the Born expansion contribute to the transport properties, smoothing out all details. For example, the kink which appears around  $V_0 = 0.7$  in the dashed line of Fig. (2), due to the speci-

ficity of the potential correlation function [16], is no longer visible in the “exact” numerical results.

For a symmetric Gaussian distribution of potential  $P_{\text{Gauss}}(V) = \exp(-V^2/2V_0^2)/\sqrt{2\pi V_0^2}$ , the mobility edge, shown in table II, is similar for various correlation functions, around -0.13, but significantly different from the blue and red speckles, although the current implementation of the SCTL gives exactly the same value for the three distributions, around -0.074.

The failure of the SCTL is mainly due to the use of the lowest order in the Born approximation. The large red-blue difference unambiguously demonstrates that odd powers of  $V_0$  (absent for a Gaussian distribution) play a major role. But even when such terms are absent, the SCTL is not very accurate. We thus believe that inclusion of higher order terms – even approximately – is a necessary step to make these theories more reliable.

To summarize, we have shown that it is possible to numerically compute the mobility edge for cold atoms exposed to a disordered potential created by a 3D optical speckle. The calculation is quasi-exact (limited only by computer resources) and its accuracy largely sufficient for comparison with experimental results. The mobility edge for a blue-detuned speckle is very significantly lower than predicted by the self-consistent theory of localization. We attribute the difference to the peculiar potential distribution of the speckle, while the spatial correlation function defines the characteristic energy scale  $E_\sigma$  but seems otherwise to play a rather minor role. While we have used for simplicity an isotropic disorder correlation function, the method can be extended to the more anisotropic configurations used in the experiments. This problem is currently under investigation.

We thank N. Cherroret, C. Müller, B. Shapiro and S. Pilati for useful discussions. This work was granted access to the HPC resources of TGCC under the allocation 2013-056089 made by GENCI (Grand Equipement National de Calcul Intensif) and to the HPC resources of The Institute for scientific Computing and Simulation financed by Region Ile de France and the project Equip@Meso (reference ANR-10-EQPX- 29-01).

- 
- [1] P. W. Anderson, Phys. Rev. **109**, 1492 (1958).
  - [2] P. A. Lee and T. V. Ramakrishnan, Rev. Mod. Phys. **57**, 287 (1985).
  - [3] D. S. Wiersma, P. Bartolini, A. Lagendijk, and R. Righini, Nature (London) **390**, 671 (1997).
  - [4] M. Störzer, P. Gross, C. M. Aegerter, and G. Maret, Phys. Rev. Lett. **96**, 063904 (2006).
  - [5] T. Schwartz, G. Bartal, S. Fishman, and B. Segev, Nature (London) **446**, 52 (2007).
  - [6] Y. Lahini, A. Avidan, F. Pozzi, M. Sorel, R. Morandotti, D. N. Christodoulides, and Y. Silberberg, Phys. Rev. Lett. **100**, 013906 (2008).

- [7] H. Hu, A. Strybulevych, J. H. Page, S. E. Skipetrov, and B. A. van Tiggelen, *Nat. Phys.* **4**, 945 (2008).
- [8] A. A. Chabanov, M. Stoytchev, and A. Z. Genack, *Nature (London)* **404**, 850 (2000).
- [9] J. Billy, V. Josse, Z. Zuo, A. Bernard, B. Hambrecht, P. Lugan, D. Clément, L. Sanchez-Palencia, P. Bouyer, and A. Aspect, *Nature (London)* **453**, 891 (2008).
- [10] G. Roati, C. d’Errico, L. Fallani, M. Fattori, C. Fort, M. Zaccanti, G. Modugno, M. Modugno, and M. Inguscio, *Nature (London)* **453**, 895 (2008).
- [11] F. L. Moore, J. C. Robinson, C. F. Bharucha, B. Sundaram, and M. G. Raizen, *Phys. Rev. Lett.* **75**, 4598 (1995).
- [12] J. Chabé, G. Lemarié, B. Grémaud, D. Delande, P. Szriftgiser, and J. C. Garreau, *Phys. Rev. Lett.* **101**, 255702 (2008).
- [13] M. Lopez, J.-F. Clément, P. Szriftgiser, J. C. Garreau, and D. Delande, *Phys. Rev. Lett.* **108**, 095701 (2012).
- [14] S. S. Kondov, W. R. McGehee, J. J. Zirbel, and B. DeMarco, *Science* **334**, 66 (2011).
- [15] A. Yedjour and B. A. Tiggelen, *Eur. Phys. J. D* **59**, 249 (2010).
- [16] M. Piraud, L. Pezzé, and L. Sanchez-Palencia, *New Journal of Physics* **15**, 075007 (2013).
- [17] D. Vollhardt and P. Wölfle, in *Electronic Phase Transitions*, edited by Hanke, W. and Kopaev Yu. V. (Elsevier, 1992), pp. 1–78.
- [18] F. Jendrzejewski, A. Bernard, K. Müller, P. Cheinet, V. Josse, M. Piraud, L. Pezze, L. Sanchez-Palencia, A. Aspect, and P. Bouyer, *Nat. Phys.* **8**, 398 (2012).
- [19] M. Piraud, Ph.D. thesis, Université Paris Sud (2012).
- [20] J. Goodman, *Speckle Phenomena in Optics: Theory and Applications* (Roberts & Company Publishers, Dover, Englewood, Colorado, USA, 2007).
- [21] A. McKinnon and B. Kramer, *Z. Phys. B* **53**, 1 (1983).
- [22] K. Slevin and T. Ohtsuki, *New Journal of Physics* **16**, 015012 (2014).
- [23] R. Kuhn, Ph.D. thesis, Bayreuth and Nice Universities (2007).
- [24] R. Kuhn, O. Sigwarth, C. Miniatura, D. Delande, and C. Müller, *New J. Phys.* **9**, 161 (2007).
- [25] J. Kroha, T. Kopp, and P. Wölfle, *Phys. Rev. B* **41**, 888 (1990).
- [26] S. Pilati, S. Giorgini, and N. Prokof’ev, *Phys. Rev. Lett.* **102**, 150402 (2009).
- [27] S. Pilati, S. Giorgini, M. Modugno, and N. Prokof’ev, *New Journal of Physics* **12**, 073003 (2010).
- [28] For a blue speckle, there is a strict lower bound  $-V_0$  for the energy spectrum, but the density of states is vanishingly small just above  $-V_0$ . For a red speckle, the energy spectrum is unbounded.